TRANSACTIONS OF THE INSTITUTE OF FLUID-FLOW MACHINERY

No. 131, 2016, 97–109

Kiryll Kabalyk*, Władysław Kryłłowicz

Numerical modeling of the performance of a centrifugal compressor impeller with low inlet flow coefficient

Institute of Turbomachinery, Lodz University of Technology, 219/223 Wólczańska, 90-924 Łódź, Poland

Abstract

The paper presents the results of computational fluid dynamics modeling of the performance of two centrifugal impellers with low inlet flow coefficients. The first impeller with the flow coefficient of 0.024 had nine main and nine splitter blades and the outlet diameter of 447 mm. The second one differed from the first one only by the lack of the splitters, 18 main blades were used instead. The numerical simulations were verified by the experimental measurements performed on a corresponding test rig. The measurements show better performance characteristics of the impeller with splitters. The main aim of the numerical research, therefore, was to identify the reasons for the existing differences in the performance of the impellers.

Keywords: Centrifugal compressor; Low flow coefficient

Nomenclature

b	–	blade height, mm
c	–	flow velocity, m/s
D	–	diameter, mm
h	–	head, J/kg
p	–	pressure, Pa
T	–	temperature, K
$\dot{m}$	–	mass flow rate, kg/s
M_{u2}	–	specific Mach number estimated on the basis of the impeller tip speed u_2
$y+$	–	dimensionless number characterizing the Reynolds number value computed at 'first-to-wall' mesh node

*Corresponding Author. Email address: kirill.kabalyk@p.lodz.pl

u – tangential velocity, m/s
w – relative velocity, m/s

Greek symbols

ζ – loss coefficient
η – efficiency
μ – viscosity, Pa s
Π – pressure ratio
Φ – flow coefficient
Ψ – head coefficient

Subscripts and superscripts

h – hub
i – internal
imp – impeller
in – inlet
s – isentropic
spl – splitter
T – theoretic
t – turbulent
tot – total
u – circumferential projection, related to the impeller tip speed u_2
$wall$ – wall
0 – stage inlet
1 – impeller inlet
2 – impeller outlet
3 – diffuser inlet
4 – diffuser outlet
* – refers to total parameters

1 Introduction

The so-called centrifugal impellers with low flow coefficients are typically employed in applications when the ratio between the volume flow rate at the stage inlet to the product of impeller's outlet diameter and outlet tangential velocity reaches the values from 0.010 to 0.025 [1]. Commonly, the wheels of this type operate at the last stages of multistage single shaft centrifugal compressors with discharge pressures of 10 MPa and higher [3].

When looking at the meridional cross section of a multistage centrifugal compressor utilized, e.g., for the purposes of the chemical industry, the low flow coefficient stages might be identified by low relative heights of their impellers (b_2/D_2) and radial diffusers (b_4/D_2). Coming out from a desire to maintain the meridional flow velocity at a sensibly high level these narrow channels on the other hand represent the first source of an inability of such type of stages to operate at

efficiencies close to 0.8–0.9, typically accepted as normal ones for higher b_4/D_2. The decrease of impeller and diffuser heights brings lower hydraulic diameters of the channels of these elements and consequently provokes the rise of the friction losses [4].

Another reason for poorer performance of low flow coefficient stages is known to stem from losses due to impeller disk friction and leakages through labyrinth seals. These are known to rise counter proportionally to the flow coefficient [5].

Over the last six decades the researchers have been searching for possibilities to improve the performance of stages operating at low Φ. The study reported by Casey *et al.* [4], for instance, discovered that higher pressure ratios might be achieved in impellers with higher outlet blade sweep, which might seem controversial to a general rule for turbocompressors that is typically derived from Euler's equation

$$h_T = c_{u2}u_2 - c_{u1}u_1 \ , \tag{1}$$

where c_{u2} and c_{u1} are the circumferential flow velocities at impeller outlet and inlet respectively, u_2 is the impeller tip speed, and u_1 is the tangential velocity at impeller inlet. In this paper, the focus is put on the application of computational fluid dynamics (CFD) in order to see how might a wider throat of the impeller with splitters alter the performance characteristics of the stage.

2 Experimental test rig

Setting up the object of investigation for the current research it was decided to choose the one that will provide the possibility of experimental verification of numerical computations. Due to the fact that in the late 90s a set of performance tests for low flow coefficient stages has been carried out in the Institute of Turbomachinery, Lodz University of Technology, the corresponding test rig was chosen for this study. The compression module of the test rig in its meridional cross-section as well as the photo of the whole installation are presented in Figs. 1a and 1b, respectively. The main geometric parameters of the compression stage defined in Fig. 1a are listed in Tab. 1 in dimensionless fashion.

The shrouded impeller 447 mm in outlet diameter possessed nine main and nine splitter blades rotating at 10175 rpm resulting in the outlet tip speed of $u_2 = 238$ m/s or $M_{u2} = 0.7$. The compression stage was connected to the suction system upstream the inlet guide vanes (IGV) and to the outlet collector at the outlet of the vaneless diffuser (VLD). The suction system comprised a circular pipeline with a mass flow measurement orifice installed inside. The pipeline was connected to the laboratory premises from the inlet and to the large inlet plenum

at the outlet. The latter played a role of a linking member between the pipeline and the stage.

Employing the scheme of the control sections given in Fig. 1a the measurements of the main thermodynamic operational parameters were organised following the next procedure:

- section '0–0' – measurement of total temperature, total pressure, static pressure;
- section '2–2' – measurement of static pressure;
- section '4–4' – measurement of total temperature, total pressure, static pressure.

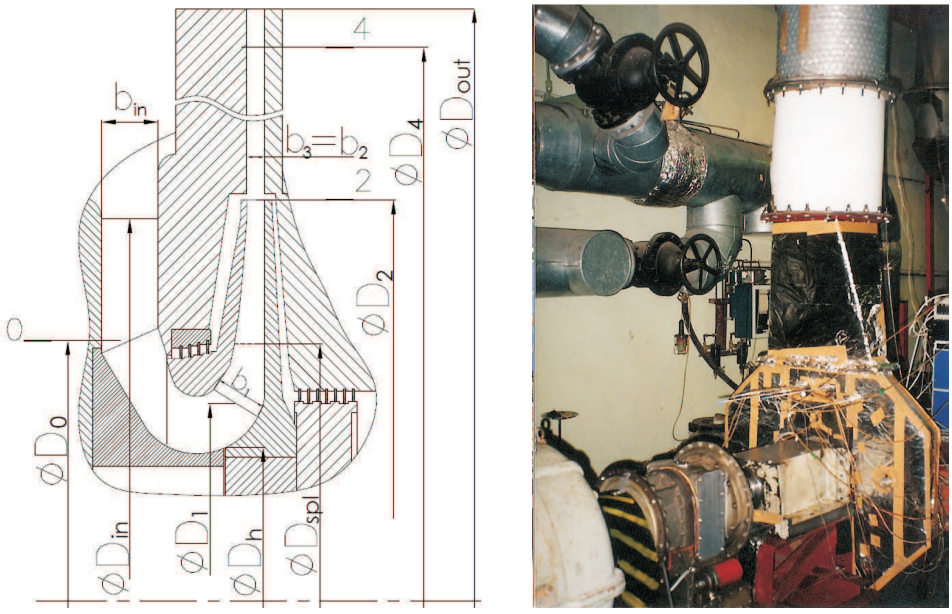

(a) (b)

Figure 1: Sketch of the meridional cross-section (a) and the photograph (b) of the "127" test rig developed at IT TUL, 1997.

Table 1: Main geometric parameters of the '127' compression stage.

D_2, mm	D_{in}/D_2	D_0/D_2	D_h/D_2	D_1/D_2	D_{spl}/D_2	D_4/D_2	D_{out}/D_2	b_2/D_2	b_{in}/b_2	b_1/b_2	b_3/b_2
447	0.95	0.65	0.38	0.49	0.64	1.38	1.48	0.02	3.2	2.9	1.0

3 Development of a numerical model

A steady-state RANS-based Ansys CFX 16.2 solver [www.ansys.com] was chosen as a computational environment. The computational domain for the 'splitted' (with splitters) impeller is shown in Fig. 2. A similar one was created for the case of the 'unsplitted' (fully-bladed) wheel. The domain includes three flow passages: the IGV passage, the impeller passage and the VLD passage. In order to reduce the computational power requirements it was decided to simulate the flow through only two blade passages applying the rotational periodicity boundary condition onto the circumferential boundaries. Each of the finite volumes of the domain was set to possess the properties of air in its calorifically perfect state ('air ideal gas'). The rotational speed of 10175 rpm was specified for the impeller passage while the IGV and the VLD were left stationary. The turbulent stresses were computed by means of two-equation k-ω SST (shear stress transport) eddy viscosity model.

The set of the boundary conditions used in the simulations was the following:

- inlet boundary – total pressure, p_{tot}, total temperature, T_{tot}, eddy viscosity ratio, $\mu_t/\mu = 10$, turbulence intensity, $Tu = 0.05$;
- hub and shroud surfaces, IGV vane, impeller blades – hydraulically smooth wall with zero velocity vector on its surface, $\vec{c}_{wall} = 0$ m/s;
- outlet boundary – mass flow rate, $\dot{m}$, kg/s.

The set of the flow parameters specified at the inlet and outlet boundaries for seven operational points chosen for the simulations is given in Tab 2.

Table 2: Boundary conditions used in numerical simulations.

Operational point	$p_{tot\,inlet}$, Pa	$T_{tot\,inlet}$, K	$\dot{m}$, kg/s	Φ
1	101325	293	0.393	0.009
2	101325	293	0.633	0.014
3	101325	293	0.729	0.016
4	101325	293	1.062	0.024
5	101325	293	1.170	0.026
6	101325	293	1.359	0.030
7	101325	293	1.557	0.035

$\Phi = 4\dot{m}/(\rho^*_{in}\pi D_2^2 u_2)$, where $\rho_{in}*$ – total density at machine inlet, D_2 – impeller outlet diameter.

The transition from stationary frame of reference to rotational one in the case of IGV-impeller interface and vice versa in the case of impeller-VLD one was realised

by means of sliding mesh approach (known as 'stage' interface model in Ansys CFX). This approach is characterised by applying the circumferential averaging to each computed flow parameter on each of the circumferential grid lines of the interface. In the case of the IGV-impeller connection the sliding mesh provided the elimination of differences in the domains' angular mutual positioning. In the case of impeller-VLD a smoother velocity profile at VLD inlet was reached, which helped to accelerate the numerical convergence of the simulations.

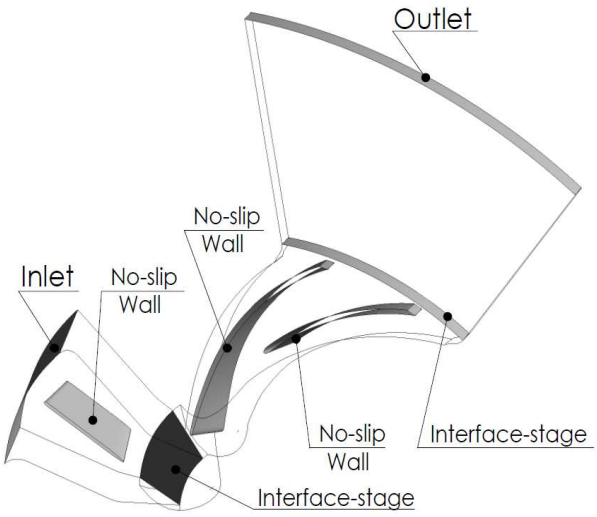

Figure 2: Computational domain for the stage with 'splitted' impeller.

The computational meshes for each of the domains were generated in Ansys CFX Turbogrid 16.2 grid generator [www.ansys.com]. The final mesh of the 'splitted' domain consisted of 690 526 hexahedral elements whereas the final size of the 'unsplitted' domain mesh constituted 553 040 elements. Both meshes were designed in order to satisfy the following qualitative requirements:

- the minimal face angle was controlled not to be lower than 20 degrees,
- the local mesh expansion factor was forced to lie within the range of 1.25–1.40,
- the maximal edge length ratio of a single mesh element was kept inside 300–600,
- the first-to-wall element height did not exceed the value of 20 μm,
- the maximal $y+$ did not exceed 20.

The mesh architecture in the vicinity of the impeller's leading edge at middle span is shown in Fig. 3a ('splitted' domain) and in Fig. 3b ('unsplitted' domain).

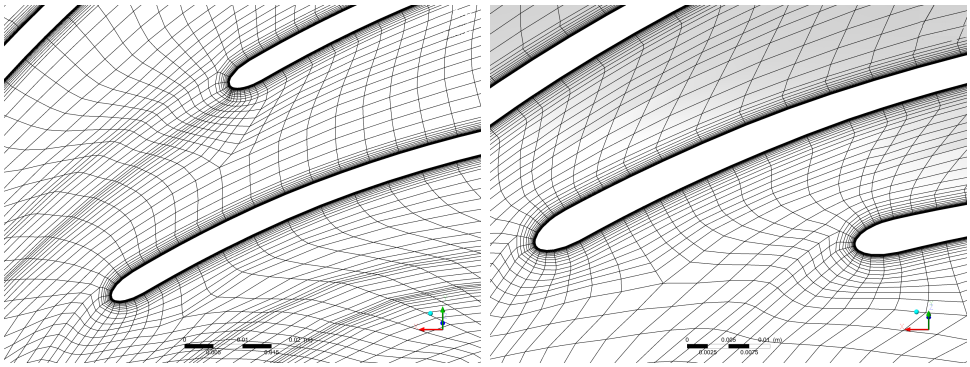

(a) (b)

Figure 3: Samples of computational mesh at the middle span surface for 'splitted' (a) and 'unsplitted' (b) impellers.

4 Results and discussion

The measured and numerically computed integral characteristics of the stage performance (Fig. 4) are going to be discussed first. Analysing the set of data shown in Fig. 4a – pressure rise maps – a good correspondence between the experimental and computational results is observed. On average, the experiment – numerical simulation (NS) deviation here fluctuates around the value of 1%, with exception for $\Phi = 0.030$ where the difference constitutes 4% in favour of NS. Comparing the numerical results to each other it is visible that the wheel with splitters provides higher pressure increase at higher flows. In a fully-bladed impeller the higher pressure ratio is reached only at the lowest mass flow rate. The isentropic efficiency map shown in Fig. 4b indicates a serious overprediction of the stage performance by the computations. The numerically obtained values of η_{s0-4} exceed the experimental ones by around 11% within almost the whole operating range of the machine. The reason for such deviation most probably lies in the incorrect modeling of the total energy losses within the vaneless diffuser introduced by a sliding mesh interface. Unfortunately, the lack of experimental data concerning the VLD flow behaviour did not allow to confirm or disapprove this hypothesis. Comparison of the numerical results shows a slightly better operation of the stage with 'unsplitted' wheel within $0.009 \leq \Phi \leq 0.016$. As $\Phi \geq 0.024$ the 'splitted' stage operates more efficiently proportionally to the increase of the flow coefficient. The internal head coefficient diagram in the Fig. 4c illustrates a good correspondence between the NS and the experiment. The existing 8–14% underprediction should result from the lack of the leakages' modeling in the accepted computational ap-

proach [1]. If so, the hypothesis concerning the cause of the discrepancies in efficiency modeling mentioned above seems to sound fairly, as the numerical error of the very impeller performance modeling should be marginal then.

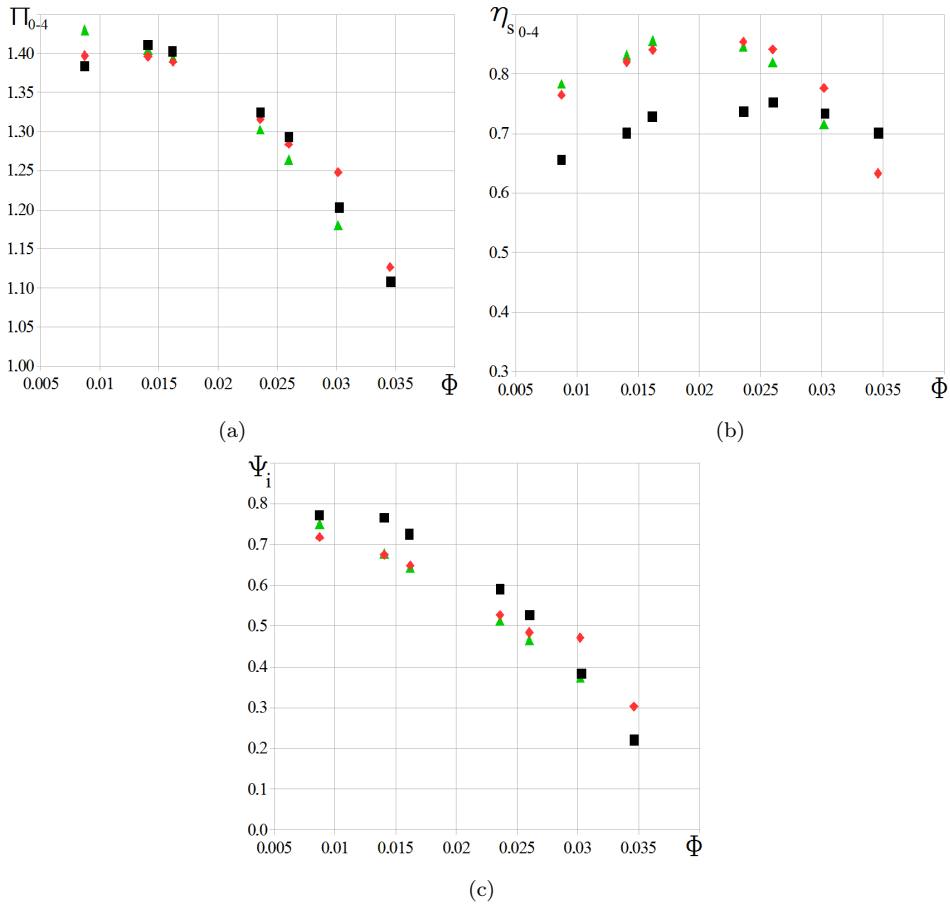

Figure 4: Dependences of stage pressure ratio Π_{0-4} (a), isentropic efficiency η_{s0-4} (b), internal head coefficient Ψ_i (c) on inlet flow coefficient Φ: squares – experiment, diamonds – impeller with splitters, triangles – fully-bladed impeller.
$\Pi_{0-4} = p_4/p_0$, $\eta_{s\_0-4} = h_{s\_0-4}/h_T$, where h_{s_0-4} – isentropic head computed on the way from section 0 to section 4, J/kg, $\Psi_i = h_i/u_2^2$, where h_i – internal head, J/kg.

The integral performance characteristics of the 'splitted' and 'unsplitted' impellers are given in Fig. 5 in terms of the impeller loss coefficient $\zeta_{imp}(\Phi)$ (Fig. 5a) and impeller total to total polytropic efficiency $\eta*_{p0-2}(\Phi)$ (Fig. 5b) dependences. The definition of the parameters might be found in [6,7]. The main visible trends are the following:

- the 'unsplitted' wheel shows a visibly better performance at lower flows ($0.009 \leq \Phi \leq 0.016$), the loss coefficients of the one are by 15–35% lower than of the 'splitted' impeller, the efficiencies, in turn, are by 1–3% higher;
- at higher flow coefficients ($0.024 \leq \Phi \leq 0.030$) the situation is reverse: the total energy losses are lower by 5–18% within the impeller with splitters whereas the efficiency of the one is by 1–8% better compared to a fully-bladed wheel.

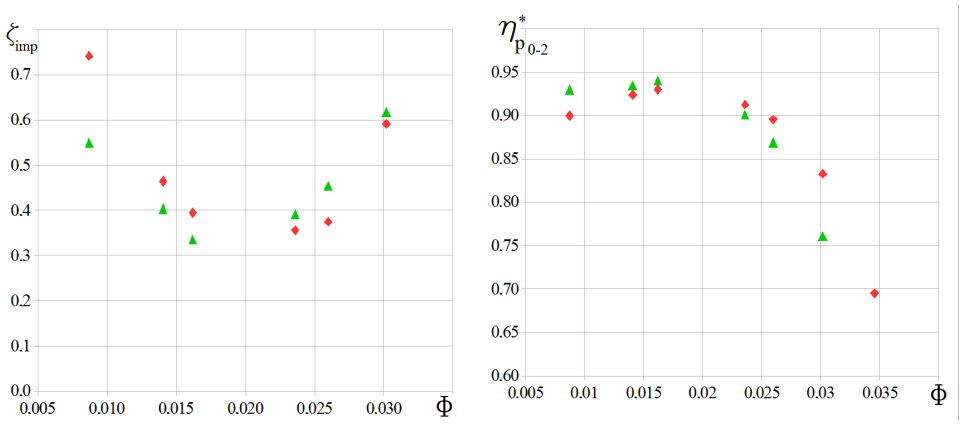

(a) (b)

Figure 5: Dependences of impeller loss coefficient ζ_{imp} (a), polytropic efficiency η_{p0-2} (b) on inlet flow coefficient Φ: diamonds – impeller with splitters, triangles – fully-bladed impeller.

Figure 6 shows the streamlines of the relative velocity vector $\vec{w}$ computed at the middle span surface for both of the impeller variants at the minimal flow coefficient of $\Phi = 0.009$. The analysis of the flow pattern of the 'splitted' impeller (Fig. 6a) indicates the existence of a flow separation zone within the vicinity of the splitter's leading edge. In the case of the fully-bladed wheel the stalled area nearby the blade suction surface is also visible, but is of a much smaller size. This to a reasonable extent describes the reason for a better performance of the 'unsplitted' impeller at this operation point reported in Fig. 5.

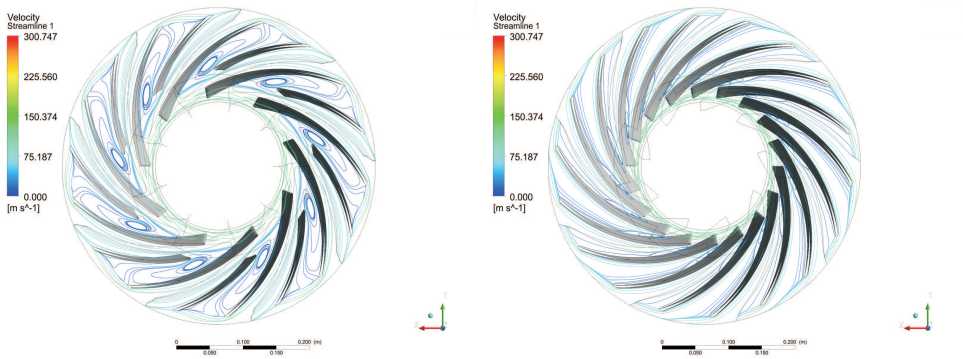

(a) (b)

Figure 6: Streamlines of the relative velocity vector computed at the middle span surface for 'splitted' (a) and 'unsplitted' (b) impellers, $\Phi = 0.009$.

Figure 7 illustrates relative velocity streamlines at middle-span at $\Phi = 0.016$. As visible, as the positive incidence gets lower, the flow pattern inside both of the impellers starts looking almost identically. The flow separation zone close to the blade suction surface mentioned above is no longer presented. The presence of any other stall cells within the impellers' channels is also hardly visible. Referring to the Fig. 5, this results in a smaller difference in impeller losses and in almost the same values of impellers' efficiencies.

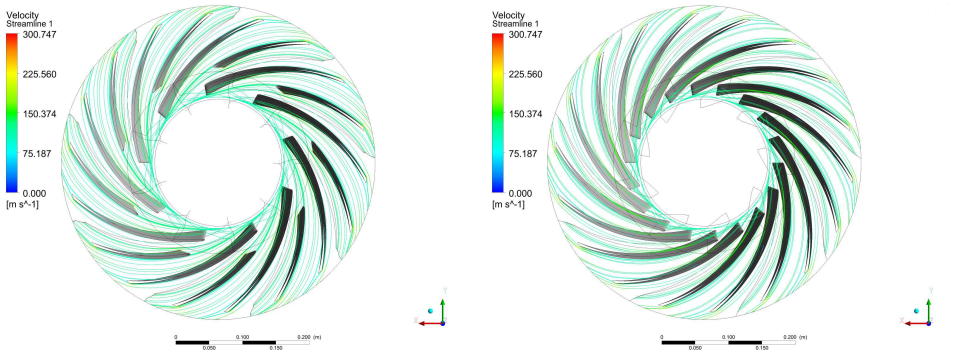

(a) (b)

Figure 7: Streamlines of the relative velocity vector computed at the middle span surface for 'splitted' (a) and 'unsplitted' (b) impellers, $\Phi = 0.016$.

As comes from Figs. 8 and 9, further increase of the mass flow rate does not bring to any severe changes in the distribution of the relative velocity throughout the

impellers. The streamlines demonstrate a smooth flux around the blades without any noticeable flow separations. In fact, the only trend that differs the computed flow patterns shown in Figs. 7–9 is the average level of velocity vector $\vec{w}$ magnitude. As expected, the higher levels correspond to the higher flow coefficients. Due to that, at a certain operating point, which according to Fig. 5 is thought to lie within $0.016 \leq \Phi \leq 0.024$, the fully-bladed wheel starts operating at lower values of efficiency and at higher loss coefficients than the 'splitted' one. The cause for the drop of the fully-bladed impeller performance is thought to outcome from two aspects:

- firstly, the increase of the velocity level at the impeller throat increases the losses due to the so-called inlet blockage, which referring to pipe-analogy might be compared to the immediate narrowing of the pipe's diameter [8];
- secondly, the total friction surface of the fully-bladed impeller is by definition higher than the one of the 'splitted' one, what results in higher friction losses of the former wheel. At flows higher than the nominal one, when the incidence is negative and typically no severe flow separations occur, friction starts playing the dominating role in defining the wheel's performance until the very choke limit [8]. As a result, the wheel with lower friction surface demonstrates lower losses then whereas the one with a higher friction surface suffers from higher total energy losses and lower efficiency.

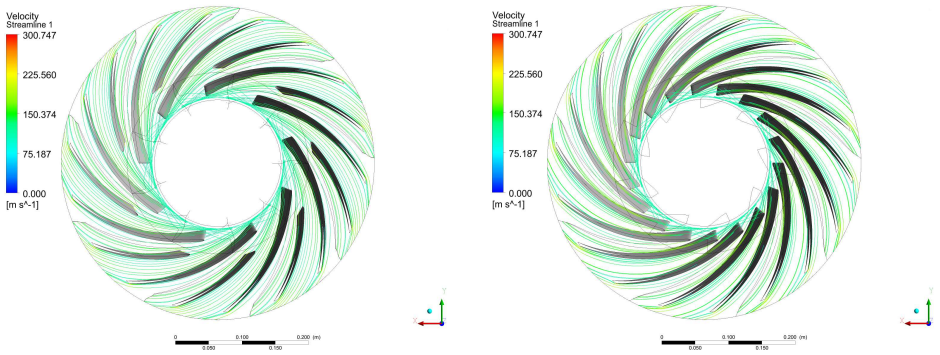

(a) (b)

Figure 8: Streamlines of the relative velocity vector computed at the middle span surface for 'splitted' (a) and 'unsplitted' (b) impellers, $\Phi = 0.024$.

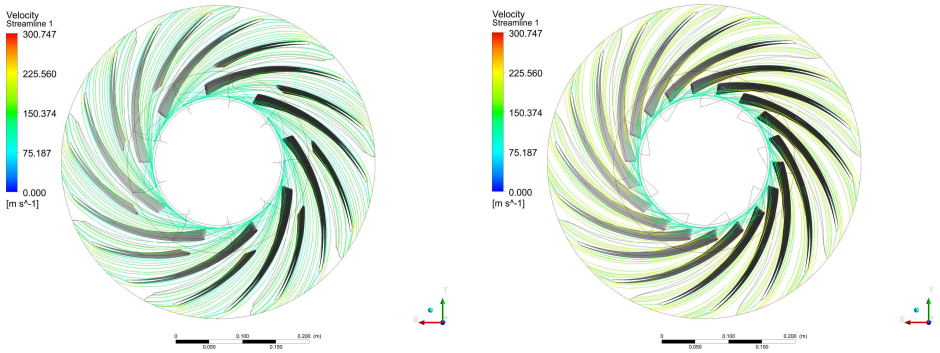

(a) (b)

Figure 9: Streamlines of the relative velocity vector computed at the middle span surface for 'splitted' (a) and 'unsplitted' (b) impellers, $\Phi = 0.026$.

5 Conclusions

A series of numerical simulations has been carried out utilizing commercial code Ansys CFX 16.2 as a computational environment in order to compare the performance of a fully-bladed and 'splitted' impellers designed for the same inlet flow coefficient of $\Phi = 0.024$ and characterized by identical geometrical characteristics. The experimental verification of the computational results was also performed applicably to the wheel with splitters. Outlining the current study, the following set of conclusions is declared:

- The numerical model showed good correspondence to the experimental measurements in terms of the prediction of the stage pressure ratio and the internal head coefficient but failed to correctly estimate the isentropic efficiency of the stage. The reason for error is thought to lie in too optimistic prediction of the flow behaviour inside the vaneless.
- The impeller equipped with 18 main blades (fully-bladed) demonstrated lower values of loss coefficients and higher values of the polytropic efficiency within the so-called region of positive incidence $0.009 \leq \Phi \leq 0.016$. However, at higher flow coefficients ($0.024 \leq \Phi \leq 0.030$) the impeller with splitters showed a better performance due to its lower total friction surface and inlet flow blockage.
- All in all, it is stated that afterwards the analysis undertaken above, it is possible to conclude that the impeller with splitters would be a better solution for an industrial application when the stage is more likely to operate at its design flow or at higher flows.

Received in July 2016

References

[1] Galerkin Yu.B.: *Turbocompressors*. SPbSPU, Saint-Petersburg 2010 (in Russian).

[2] Seleznev K.P., Galerkin Yu B., Podobuev Yu.S.: *Theory and Design of the Turbo Compressors*. Mashinostroenie, Leningrad 1986 (in Russian).

[3] Lettieri C., Baltadjiev N., Casey M., Spakovszky Z.: *Low-flow-coefficient centrifugal compressor design for supercritical CO_2*. J. Turbomach. **136**(2014), 8, 081008.

[4] Casey M.V., Dalbert P., Schurter E.: *Radial compressor stages fort low flow coefficients*. Presented at the 4^{th} European Congress on Fluid Machinery for Oil, Petrochemical and Related Industries, Imech Paper C403/004, Hague 21-23 May 1990.

[5] Dalbert P., Ribi B., Kmeci T., Casey M.V.: *Radial compressor design for industrial compressors*. In: Proc. ImechE Part C, **213**(1999), 71–83.

[6] Seleznev K.P. *et al.*: *Devising unified centrifugal compressors stages*. Chem. Petrol. Eng. **20**(1984), 108–114.

[7] Galerkin Yu.B.: *Research on Turbocompressor Making*. Chem. Petrol. Eng. **17**(1981), 469–474.

[8] Luedtke K.: *Process Centrifugal Compressors*. Springer Verlag, Berlin-Heidelberg 2004.